

## KARST SYSTEMS WITHIN THE SOUTHERN CARPATHIANS STRUCTURE (ROMANIA)

Ioan POVARĂ<sup>1</sup>, Mihai CONOVICI<sup>2</sup>, Cristian-Mihai MUNTEANU<sup>1</sup>,  
Constantin MARIN<sup>1</sup> & Elena Daniela IONIȚĂ<sup>3</sup>

<sup>1</sup>"Emil Racoviță" Institute of Speleology of the Romanian Academy, Frumoasă Street, 31, Bucharest, Romania  
ipov.iser@gmail.com

<sup>2</sup>Geological Society of Romania, Nicolae Bălcescu Avenue, 1, Bucharest, Romania

<sup>3</sup>National Mineral Water Society, Water Analysis Laboratory, Iuliu Maniu Avenue, 19, Bucharest, Romania

**Abstract.** The Cerna River catchment area is located in the south-western part of the Southern Carpathians, along the Cerna Miocene Graben, within which outcrop Cretaceous formations pertaining to either the Danubian Autochthonous or the Getic Nappe. Consequently, secondary structures characteristic to the extensional tectonics have resulted. These structures have been involved in the groundwater flow, leading to the high flow rates recorded for certain karst springs (Pișetori, Seven Cold Springs, Domogled) and to the low flow rates of several cross creeks. On the western slope of the valley, close to the master fault, the karst aquifer complex, developed within the Mesozoic limestone, is strongly influenced by thermal phenomena. Along the valley, on 25 km, to the south, towards the Băile Herculane area, 28 thermal sources (10 wells and 18 springs) have been identified. Structural and tectonic relationships between the deep-seated, brittle granitic bedrock and the limestone cover, capped by Cretaceous argillites, are very important for the dynamics of the thermo-mineral reservoir. There is a clear-cut distinction between the karst springs and the thermal sources, in terms of both hydrochemical facies, and dissolved minerals. The chemical analyses of the groundwater samples collected from the Cerna River catchment area outline clear hydrochemical differences between the karst springs and the thermo-mineral sources. In the karst groundwater, Ca<sup>2+</sup> and HCO<sub>3</sub><sup>-</sup> (up to 200 mg/L) are the prevailing ions. The thermo-mineral water is of Na-Cl type; its mineral content exhibits a markedly increasing trend from the north to the south (from 170 to 8000 mg/L). There is an obvious correlation between Na<sup>+</sup> and Cl<sup>-</sup> concentrations, indicating a mixing process between a common saline end-member and a less mineralized shallow water.

**Keywords:** Southern Carpathians, Mesozoic limestones, graben, karst systems, hydrogeochemistry.

### 1. INTRODUCTION

The Cerna River catchment area extends on over 555 km<sup>2</sup> (Fig. 1), out of which 88.56 km<sup>2</sup> (16%) are covered by Mesozoic limestones. The main landforms are represented by mountains, higher than 2200 m in the north, but only 130 m high in the south. The non-karst rocks (which outcrop on more than 400 km<sup>2</sup>) allow a permanent surface flow towards the lithological contact with the limestones, where the streams sink in the underground. The groundwater systems are discharged by karst springs with cumulated flow rates of over 10 m<sup>3</sup>/s.

According to the classification issued by Mangin (1975), the karst aquifers from the Cerna River catchment area can be assigned to either *the type III* (e.g. the Cerna Spring, with a stronger karst

behavior in the upstream sector), or *the type V* (e.g. the Pișetori Springs, the Seven Cold Springs and the Domogled Spring, with non-karst behavior).

The limestones outcropping within the area of the Băile Herculane Spa play a very important role in the functioning of the thermo-mineral aquifer.

### 2. GENERAL GEOLOGICAL DATA

The area is covered by rock formations pertaining to two main tectonic structures of the Southern Carpathians: (1) *The Getic Nappe*, which includes meso-metamorphic and Paleozoic and Mesozoic sedimentary formations, that transgressively overlie the crystalline schists of the Godeanu Mountains; (2) *The Danubian Autochthonous*, which comprises metamorphic formations intruded

by granite bodies, and also Paleozoic and Mesozoic sedimentary formations, developed in facies types different from those of the Getic Nappe.



Figure 1. Location of the study area within Romania.

The recent sedimentary cover consists of Quaternary deposits, outcropping in glacial and fluvio-glacial facies. After the Late Cretaceous collisional tectonic stage, the large Getic and Danubian structures from the SW of the Southern Carpathians have been fragmented by the transtensional-transpressional movements that were active during the Late Oligocene-Miocene. These movements led to the complex half-graben structure of the Cerna Valley. The eastern fault of the structure includes an uplifted block with high escarpment, while the western one is a strike-slip master fault, sunken along the valley. The very complex structures and morphology have created an intricate system of channels. Differences between the tectonic behavior of the granitic bedrock and the Mesozoic sedimentary cover led to “positive” and “negative flower structures”, identified on the eastern slope of the valley during our recent studies.

### 3. MATERIALS AND METHODS

The geological description follows the Geological Map of Romania (at the scales 1:200 000 and 1:50,000). We additionally performed geological surveys of the complex structures, at the scale 1:10,000. The hydrogeological characterization has been based on archived data and on our measurements. Gauging maximum flow rates smaller than 200 l/s at karst springs was carried out with either trapezoidal or triangular (45°) thin-edge weirs, while to establish the groundwater flow paths and velocities, non-polluting tracers were injected. In order to assess certain groundwater flow parameters and to categorize the karst systems, the

methodological approach of Mangin (1975, 1982) was used.

For characterizing the chemistry of various waters that occurred in the Cerna river catchment area, samples have been collected from outflows belonging to the karst systems, from the main discharge sites of the thermo-mineral water accumulation, as well as from the Cerna river course. The sampling was performed during the time-interval June-August 2013.

All bottles used for storing the collected samples were of the Nalgene High-Density Polyethylene type. When collected, the samples for the cations analysis have been filtered by using Thermo Scientific Chromacol Polyether Sulphone Syringe Filters (0.45 µm pore size). Suprapur (Merck) 65% nitric acid was used for the pH adjustment of the collected samples. In separate bottles of the same type, there have been collected the samples for analyzing the total alkalinity and the anions. When the samples were collected, the outflows temperature and pH were measured. A Crison PH 25 portable instrument has been used in order to perform all pH measurements (50 51 Electrode with integrated Temperature Probes ATC, NIST-traceable pH buffer solutions of pH 4.01 and 7.00). The water total alkalinity was determined by means of Gran electrometric titration, with a 0.05 M HCl solution (Rounds, 2006) within a time-interval of no more than 24 hours after sampling. Dissolved H<sub>2</sub>S concentration for thermal waters was measured on-site using a battery operated, portable photometer (Loviband Multi Direct) and the methylene blue method (Cline, 1969).

The complete chemical analysis of all collected water samples was conducted in the laboratory of the “Emil Racoviță” Institute of Speleology of the Romanian Academy. In the following, there are essentially indicated only the techniques utilized for analyzing the components addressed by the present paper. The Na, K, Mg and Ca concentrations were determined by means of standard inductively coupled plasma mass spectrometry (ICP-MS) method (EPA, 2007). The determinations were carried out with a NexION 300S (PerkinElmer, Shelton, CT, USA) ICP-MS instrument (Serial No. 81SN2032001), equipped with a S10 Autosampler. The calibration curves were determined starting from an Instrument Calibration Standard 1 solution provided by PerkinElmer (Part No. N9300218). The solution contains Na, K, Mg and Ca, each of them in a concentration of 5000 mg/L. The working solutions for internal standard were prepared starting from Scandium standard solution, PerkinElmer Part No. N9300148, Lot No. 18-152SCX1, (1000 mg/L).

Quality Control (QC), checking and Continuing Calibration Verification (CCV) solutions preparation used Initial Calibration Verification Standard (PerkinElmer, Cat. No. 9300224). HNO<sub>3</sub> 60% Ultrapur® (Merck, Cat. No. 101518) was used for the blanks preparation and washing solutions. The chloride ion was analyzed by an ICP-MS standard method as well, with Sc as internal standard. Sulphate concentrations have been measured by means of a turbidimetric method (Aminot, 1974) using a PerkinElmer Lambda 25 spectrometer model. All the solutions have been prepared with ultra-pure water (LaboStar TWF UV7 Ultrapure Water System, electric resistance 18.2MΩ×cm).

The total dissolved solids (TDS) content was calculated as the sum of the total dissolved-ion concentrations, by additionally making the adjustment of bicarbonate to carbonate ions (Hem, 1985).

#### 4. KARST SYSTEMS

##### 4.1. The Karst System of Cerna Spring

The Cerna Spring represents the largest karst spring of Romania, the karst system being developed across the catchment areas of three different surface

streams. The groundwater outflowing at Cerna Spring (709 m a.s.l. elevation) is collected from a recharge area of 80.62 km<sup>2</sup>; non-karst rocks outcrop on 47.85 km<sup>2</sup> (59.4%) (Fig. 2). The system is located at the NE edge of Cerna Graben, a major tectonic structure which extends up to more than 50 km along a NNE-SSW direction. The bedrock consists of granite, which is overlain by a Mesozoic sedimentary cover mainly including Urgonian limestones. The latter carbonate formation shapes a high plateau (1900-2100 m a.s.l.), having the aspect of a planation surface, assigned to the Eocene erosional surface (Niculescu, 1965). The limestones morpho-tectonic evolution led to an intensely karstified system of fractures (with a high capacity to store the rainfall water - 1,100 mm/year on average), and to sinking surface streams (with flow rates of up to 5 m<sup>3</sup>/s). The longest distance from a swallow hole to the spring is 13.3 km (Ponta et al., 1984a). Average groundwater flow velocities range from 0.88 to 1.3 km/day. Within the catchment areas of the three surface streams related to the Cerna karst spring, 198 caves and potholes located at relative elevations lower than 100 m (Ponta et al., 1984b) have been inventoried.

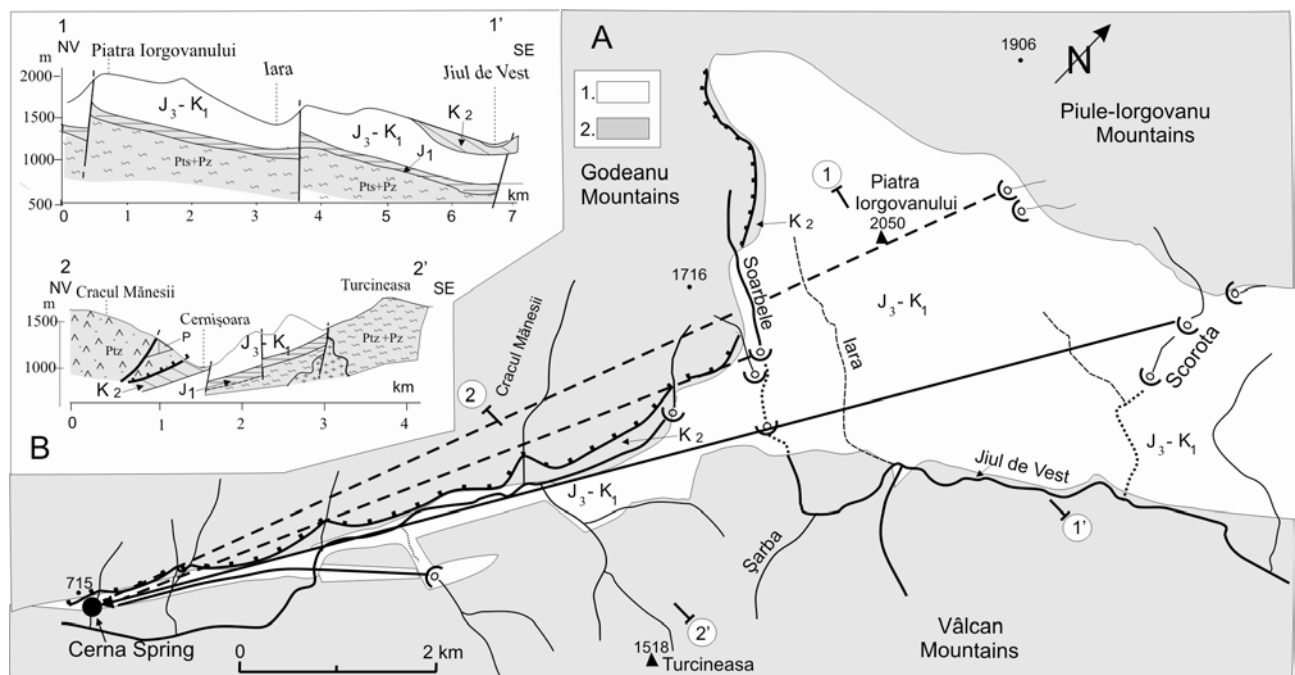


Figure 2. A. Hydrogeological map of the Jiu Valley and the Cerna Spring area : 1. Mesozoic limestones; 2. Proterozoic to Mesozoic non-karst rocks. B. 1. Upper Cretaceous argillites (mélange formations); 2. Upper Jurassic-Lower Cretaceous limestones; 3. Liassic sandstones; 4. Proterozoic granites; 5. metamorphic rocks pertaining to the Danubian Autochthonous; 6. Getic Nappe (+ Permian sandstones); 7. geological boundary; 8. fault; 9. overthrust; 10. hydrogeological cross-section line; 11. permanent surface stream; 12. temporary stream; 13. streambed seepage; 14. sinking stream; 15. dye-traced groundwater flow path; 16. hypothetical groundwater flow path; 17. mountain peak; 18. topographic elevation.

The multiannual average air temperature (5.5°C) leads to a prolonged period of frost (more than 200 days/year). The maximum water reserve stored in the snow layer (300 mm) is reached at the end of March. Consequently, the spring rainfall period (April-May) corresponds to the snowmelt, leading to maximum flow rates in the surface and the subterranean streams.

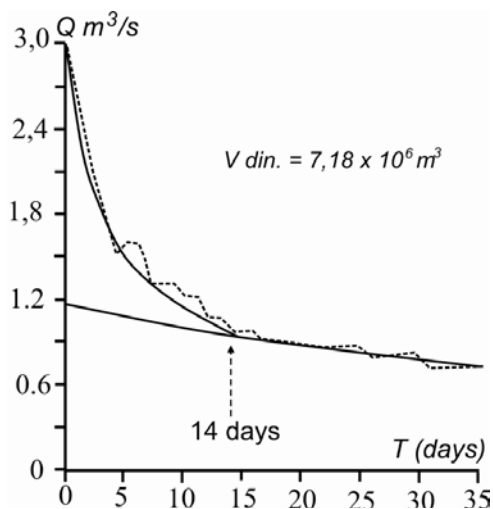


Figure 3. The Cerna Spring recession diagram for the interval 25.08.1982 – 30.09.1982.

Using the method described by Mangin (1975, 1982) - i.e. by analyzing a representative flow rate recession diagram (Fig. 3), one can notice that the flooded karst network is poorly developed, the water reserve is quickly discharged, the allogenic recharge is significant, and the water amount related to the fast infiltration is drained within a short time span (14 days).

#### 4.2. The Pișetori Karst System

The system is located within the central-northern sector of the Cerna River catchment area. It is essentially discharged by a group of 5 main springs occurring along a distance of about 100 m, at 360-386 m a.s.l. elevation. The water outflows from beneath a massive deposit of travertine, along a fault marking a boundary between the Lower Cretaceous limestones (developed in Urganian facies) and the Upper Cretaceous (Turonian-Senonian) flysch deposits. The limestone deposits cover 1.13 km<sup>2</sup>, representing 56% of the total groundwater recharge area (2.01 km<sup>2</sup>).

Within this area, the Cerna Valley left slope consists of formations belonging to the central sector of the Danubian Autochthonous, from the limit between the upper and the lower Danubian units (Săndulescu, 1984). A particular feature of the Cerna Valley left slope is the presence of the Upper Cretaceous mélangé formation, outcropping on both

sides of the river: large Lower Cretaceous limestone blocks, embedded in a matrix consisting of centimetric fragments of clay (tectonosoma), cemented by a limestone binder (Fig. 4 A, B).

From a maximum altitude of 1445 m (Vf. lui Stan), down to the Cerna River streambed (350 m a.s.l.), the slope, marked by 3-4 successive ledges (“negative flower structure”) is descending in a stepwise manner. Between the ledges, thin and elongated limestone bands, crossed by creeks (Török-Oance & Ardelean, 2012), form narrow and deep gorges, where the surface water flow is partly or completely sinking, depending on the rainfall amount. The characteristic flow rates of the springs for the interval 08.04.2005-17.03.2006 were  $Q_{\min} = 19.2$  l/s;  $Q_{\max} = 124.8$  l/s;  $Q_{\text{med}} = 48$  l/s. Over the same period, the water temperature has varied between 8.9 and 9.6°C (for comparison, the annual average air temperature was 7.1°C). The average groundwater flow velocities (computed between the diffuse sinking points of the streams and the corresponding outlets) fall within the range 0.15-0.216 km/day, typical for a deep flow along poorly karstified fractures.

The flow rate recession diagram (Fig. 5) shows that the influence of the water input resulting from the 2005 spring season snowmelt ceases 26 days after the end of the melting period; subsequently, the karst aquifer discharges only the base-flow amount.

The low value of the base-flow coefficient (the recession coefficient),  $\alpha = 0.00795$ , points to a slow groundwater flow, through fissures and small karst voids less affected by the widening process due to karst dissolution.

#### 4.3. The Seven Cold Springs Karst System

This karst system is located within the central-southern sector of the Cerna Valley, and it is supplied by seepage into the Cerna riverbed and by infiltration in the limestone plateau from the top of the slope (Fig. 6 A). The granite bedrock of the region exhibits two axial bulges (the tectonic windows Balta Cerbului and Roșeț), overlain by Lower Cretaceous limestones and by Upper Cretaceous clastic-shaly deposits.

The thin-skinned tectonics controls the groundwater flow through the limestones between the Vf. lui Stan-Domogled main anticline and the Roșeț axial bulge. Seven springs emerge from beneath the Cerna lower terrace deposits, being distributed along a distance of 80 m, on a lineament parallel with the river (Fig. 6 B).

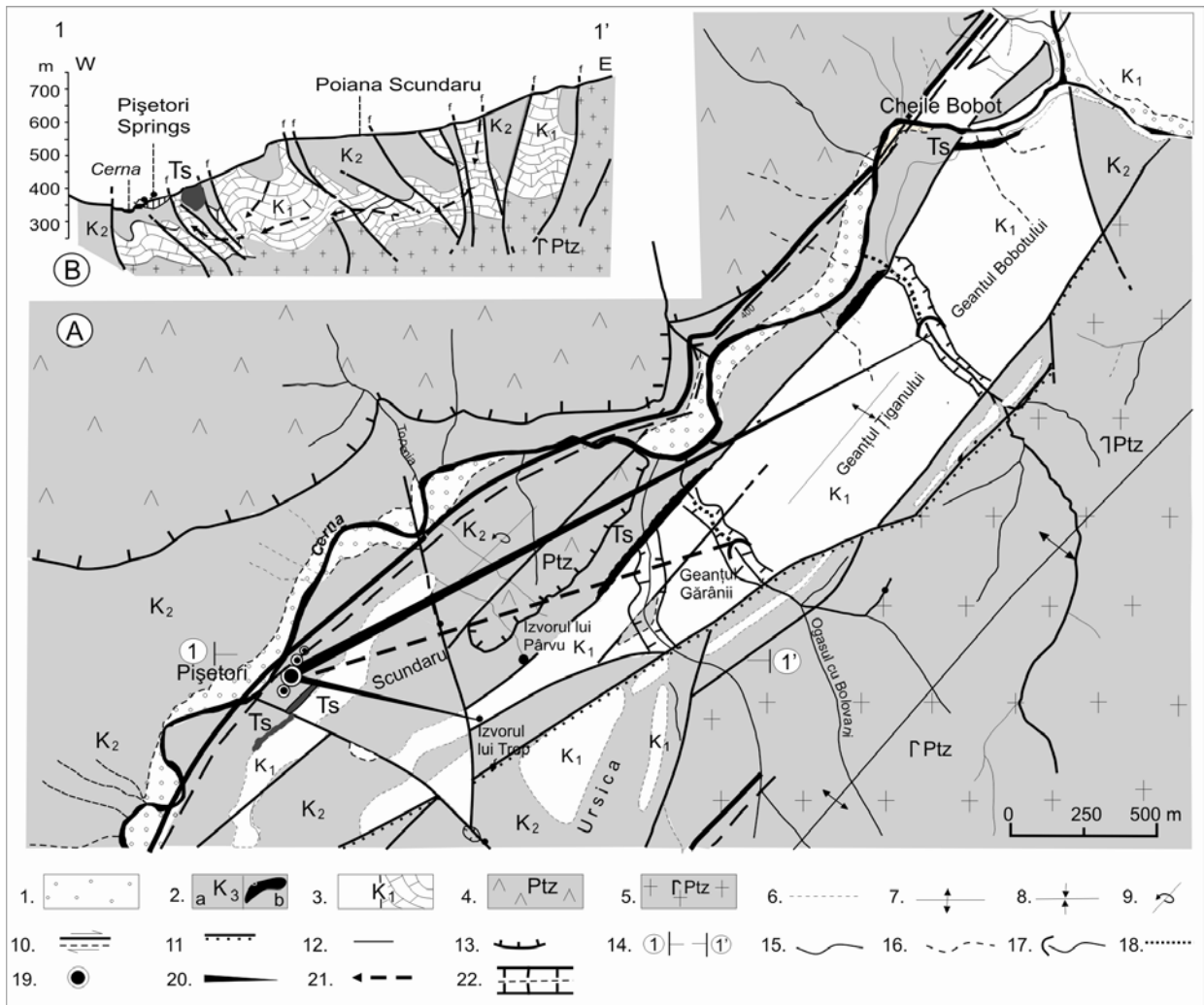
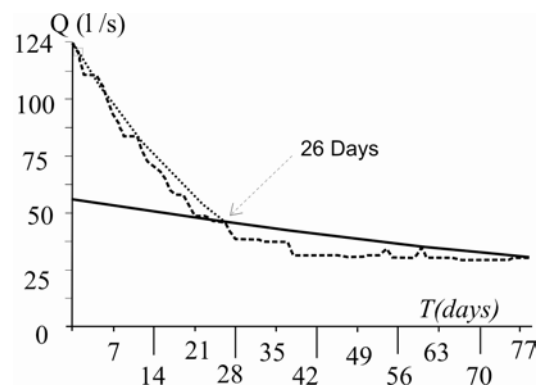


Figure 4. A. Geological and hydrogeological map of the sector Pișetori Springs-Arșasca of the Cerna Valley (after Conovici et al., 2013, simplified). B. Hydrogeological cross-section. 1. Holocene alluvia; 2. black shales with limestone olistoliths (a), Lower Cretaceous limestone tectonosomes (b); 3. Lower Cretaceous limestones; 4. Getic Nappe (retromorphic Alpine gneisses and micaschists); 5. Arșasca granites; 6. geological boundary; 7. anticline; 8. syncline; 9. secondary reversed anticline; 10. strike-slip master fault (with the area of ductile deformation and shear direction); 11. uplifted hanging wall of a reverse fault; 12. normal fault; 13. nappe boundary; 14. hydrogeological cross-section line; 15. permanent surface stream; 16. temporary surface stream; 17. sinking stream; 18. streambed seepage; 19. spring; 20. dye-traced groundwater flow path; 21. hypothetical groundwater flow path; 22. gorges.

Figure 5. Flow rate recession diagram of the Pișetori Springs for the interval 09.04.2005-17.03.2006 (With additions after Conovici et al., 2013).



The physical-chemical properties of all the outlets are similar, suggesting that a common conduit is progressively supplying them. Since 1988,

the springs discharge beneath the Herculane reservoir water level (Fig. 6 C). Therefore, the groundwater flow characterization relies on older

flow rate and rainfall data, recorded in various archives, covering the interval 17.03.1966-16.05.1967, as well as on previous dye-tracer tests (Povară & Lascu, 1978). The accordingly derived average velocities of the groundwater flow ranged between 1.1 and 1.6 km/day, while the cumulated spring flow rates varied from 110 to 336 l/s.

Due to the overflowing of the springs by the Herculane Reservoir (after 1988), we performed the analysis of a recession diagram derived from archive-based data, covering the interval 03.1966-02.1967 (Fig. 7). The results outline the significant role played by the Cerna River supply ( $i = 0.86$ ).

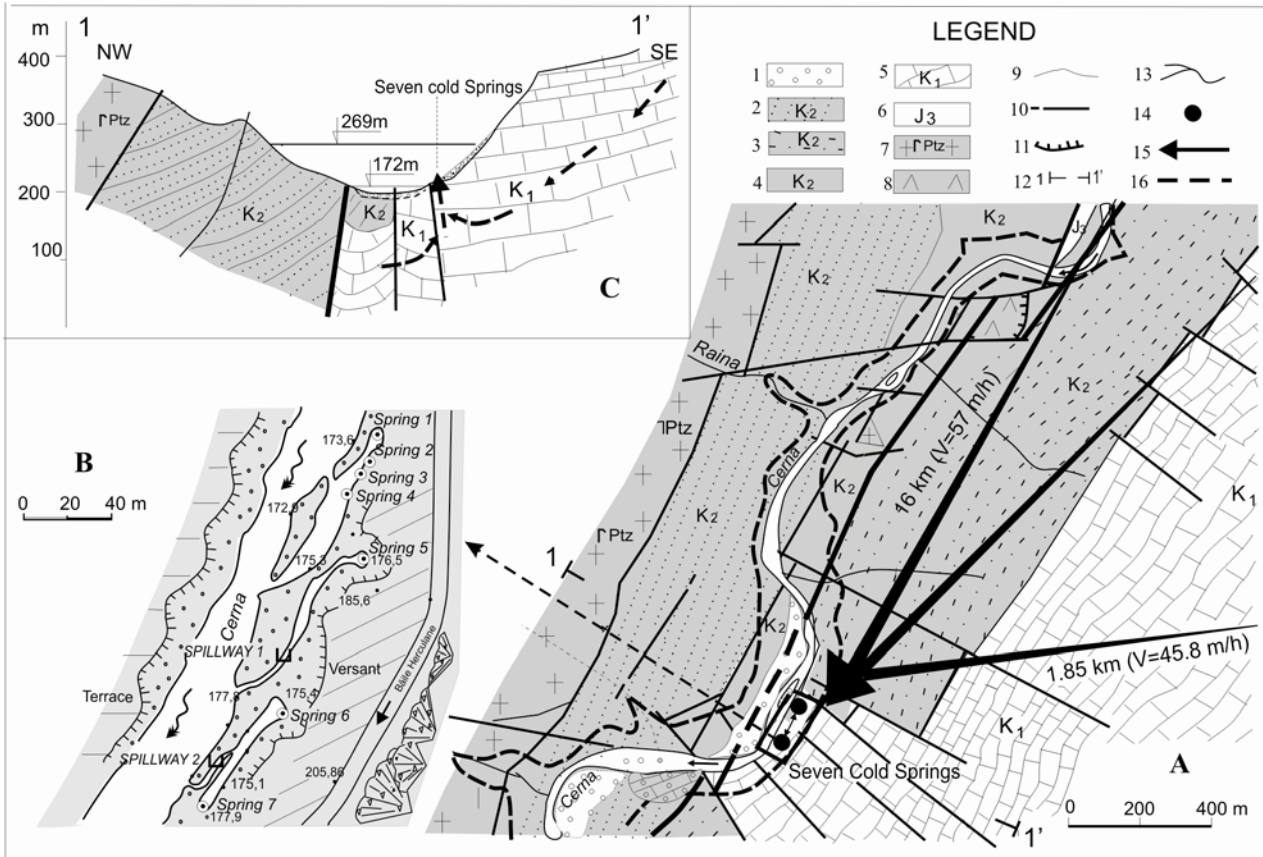


Figure 6. A. Hydrogeological map of the Seven Cold Springs area. B. Detail of the hydrogeological setting prior to the filling of the reservoir. C. Hydrogeological section (after Povară, 2012, modified): 1. Quaternary alluvia; 2. Arjana-type sandy wildflysch; 3. Cerna-type clayey wildflysch; 4. black marly limestones (the Iuta Formation); 5. Lower Cretaceous Urgonian limestones; 6. Presacina-type Upper Jurassic micritic limestone; 7. Precambrian granites; 8. metamorphic outlier pertaining to the Getic Nappe; 9. geological boundary; 10. fault; 11. overthrust; 12. hydrogeological cross-section line; 13. permanent surface stream; 14. karst spring; 15. dye-traced groundwater flow path; 16. reservoir outline.

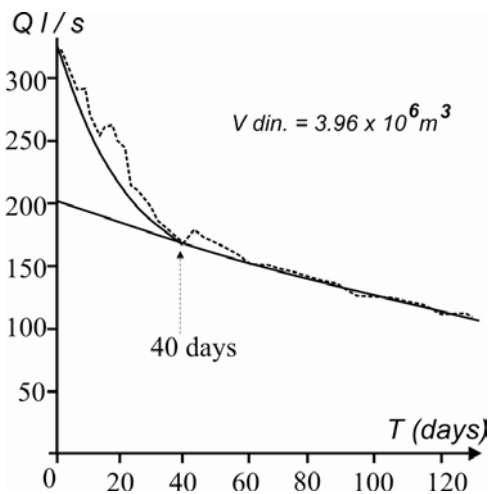


Figure 7. Flow rate recession diagram of the Seven Cold Springs for the interval 03.1966-02.1967 (after Povară, 2012).

The increase of the river flow rate leads to a higher spring discharge rate, lasting for 4 days. The recharge derived from the Cerna Valley left slope is less important and it does not significantly influence the spring flow rates.

#### 4.4. The Domogled Karst System

The karst system is located in the SE sector of the Cerna Graben. In that area, the geological structure presents an axial bulge (elevation: 700 m a.s.l.), developed on granites, overlain by Urgonian limestones, descending stepwise towards the Cerna riverbed (“negative flower structure”). To the south, the limestones are covered by Late Cretaceous clastic deposits and by metamorphic rocks belonging to an outlier of the Getic Nappe. The groundwater flows in a karst regime, towards the outlet, located underneath a colluvial deposit, at the boundary with the metamorphites pertaining to the Getic Nappe (Fig. 8).

The spring is supplied by two swallow holes,

located on the Cerna Valley left slope, at an elevation of 760-790 m a.s.l. The average groundwater flow velocity is 0.81 km/day. The recession curve, recorded during the interval 8.05.1990 – 5.10.1990, shows that the peak flow decay lasted for 112 days and was followed by a 63 days long base-flow decline (Fig. 9).

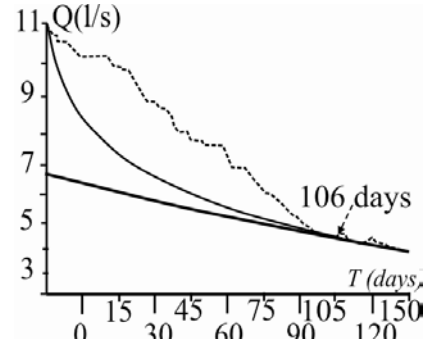


Figure 9. Flow rate recession diagram of the Domogled Spring for the interval 8.05.1990 – 5.10.1990 (after Povară, 2012).

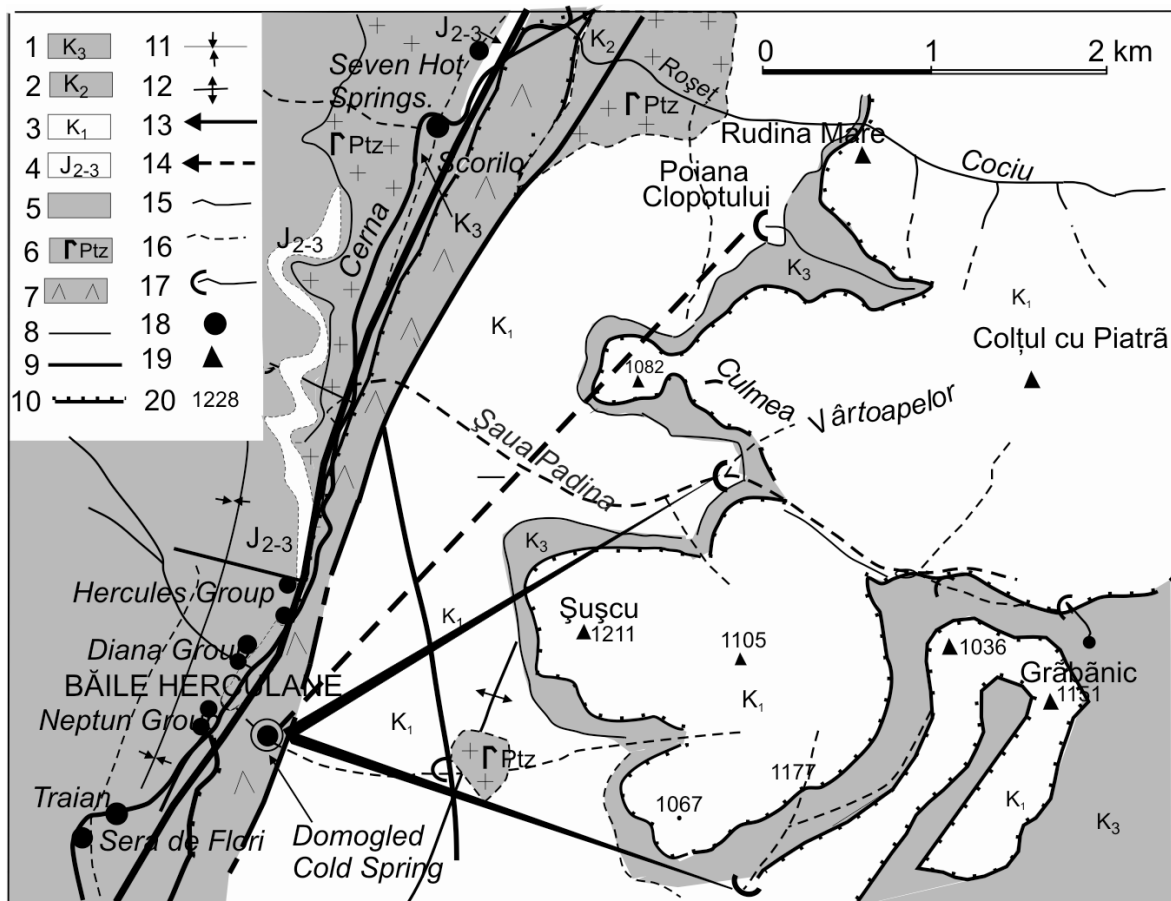


Figure 8. Hydrogeological map of the Domogled-Roșeț Area (after Povară, 2012, modified): 1. Upper Cretaceous mélanges formation (wildflysch); 2. Iuta Formation (turbiditic limestones); 3. Lower Cretaceous (Urgonian) limestones; 4. Middle-Upper Jurassic sub-lithographic limestones; 5. Upper Paleozoic-Lower Jurassic sedimentary cover; 6. Proterozoic granitoids; 7. Proterozoic metamorphic rocks (Getic Nappe); 8. geological boundary; 9. fault; 10. local overthrust; 11. syncline; 12. anticline; 13. dye-traced groundwater flow path; 14. hypothetical groundwater flow path; 15. permanent surface stream; 16. temporary stream; 17. sinking stream; 18. thermal sources and wells; 19. mountain peak; 20. topographic elevation.

#### 4.5. The Thermal System from the Băile Herculane Area

A complex aquifer system, hosted by carbonate rocks, influenced by geothermal phenomena, is located within the Cerna Graben, down to the southern boundary of the Cerna Syncline. The geothermal research in several areas (Piatra Pușcată, Crucea Ghizelei, Băile Herculane and Pecinișca), pointed to geothermal gradients ranging between 110 and 200°C/km and to temperatures varying between 13.8 and 16°C, at a depth of 30 m. Thermo-mineral springs, with different flow rates and physical-chemical properties, emerge in the studied areas. The geothermal flux significantly exceeds the country average (70-92 mWm<sup>-2</sup>) and its maxima have been mainly recorded on faults transverse to the graben (Veliciu, 1978). The geothermal flux increases especially within the sector comprised between the Băile Herculane railway station and the Crucea Ghizelei Well. The behavior of this aquifer is directly influenced by the carbonate rocks.

Due to the tectonic activity subsequent to the Jurassic-Cretaceous cycle, the limestones outcrop at various elevations: 1100 m a.s.l. in the Mehedinți Mountains, 150-600 m a.s.l. in the Cerna Syncline, or deeply sunken into the Cerna Graben, down to depths of more than 1000 m, along a transcrustal faults system. Long-range, horizontal and vertical, hydrodynamic connections have been locally established between the limestones outcropping along

the graben and on the adjacent slopes (Năstăseanu, 1980). The hydrostructures developed on the slopes often supply the graben, while the two-way water exchanges are far less frequent. Several hypothermal springs with smaller TDS contents suggest that the thermal water reservoir is extended from Piatra Pușcată (to the north) down to Topleş (to the south).

Along the graben, the reservoir has been developed within both the karstified Jurassic limestones and the weathered and fractured Cerna granites, while within the Cerna Syncline, only the karstified Jurassic limestones host thermal water (Fig. 10). The physical-chemical properties of the water vary, depending on the reservoir lithology:

- within the limestones the cold and weakly mineralized water follows a descending trajectory, as pointed out by the geoelectric investigations (Mitrofan et al., 2008), while the hot and strongly mineralized water ascends through fractures and karst voids;

- within the granites, the hot, strongly mineralized, radioactive water flows through the network of fractures and faults.

The limestones deeply sunken within the Cerna Graben, overlain by non-karst deposits, display the characteristics of a confined aquifer. Consequently, an artesian behavior (the water level rising up to 30-52 m above ground) was recorded at all the wells drilled within the graben reservoir rocks.

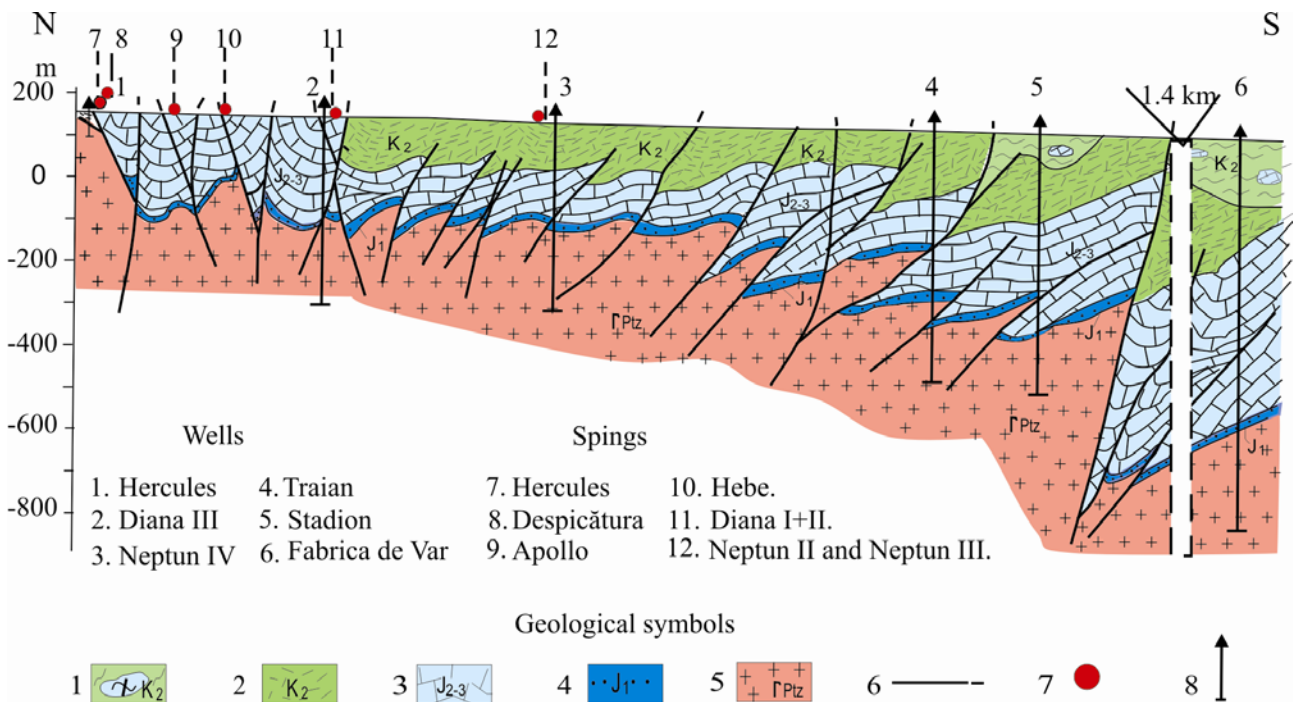


Figure 10. Longitudinal geological cross-section along the sector of the Cerna Valley affected by hydrothermal phenomena: 1. Presacina-Arjana-type wildflysch formation: ophiolites in a sandy-shale matrix; 2. Middle Cretaceous turbiditic limestones; 3. Middle-Upper Jurassic sandy limestones and micritic, nodular limestones; 4. Liassic sandstones (Gresten facies); 5. Proterozoic granites pertaining to the Danubian Autochthonous; 6. faults; 7. natural thermal springs; 8. wells.

The tests performed in the wells Crucea Ghizelei, Traian and Neptun have shown that the highest flow rates (172-691 m<sup>3</sup>/day, hence 1.99-7.99 l/s) were yielded by the karstified Jurassic-Cretaceous limestones. The maximum cumulated flow rate discharged by the springs and wells is – according to gauging operations conducted after 1984 – in excess of 90 l/s, the largest values being recorded at Hercules spring (Mitrofan et al., 2014).

According to the gauging operations carried out after 1984, the maximum cumulated flow rate discharged by the springs and wells exceeds 90 l/s, the highest values being recorded at the Hercules Spring.

## 5. RESULTS AND DISCUSSIONS

Within the highly complex “Cerna Graben” tectonic system, the karst and the thermo-mineral water follows relatively diverse flow paths. Dye-tracing tests have furthermore pointed out that the neighboring structures significantly influence the groundwater flow. For instance, the karst water derived from the Piule high plateau outflows at the Cerna Spring, located in a sector of the Cerna Graben characterized by the presence of narrow limestone “bars”. The chemical composition and the general features of the thermal water from the southern part of the Băile Herculane Spa suggest possible inflows from the adjacent geological structures, subjected to a more complex evolution.

The investigations carried out on the Cerna Valley allowed us to delineate the catchments of the most important karst springs, supplied by sinking streams. We described a series of binary karst systems, developed in Jurassic-Cretaceous

limestones, which outcrop on 15-59% of the total catchment area. The hydrostructures range from well-developed karst aquifers to non-karst aquifers, similar to the fissured aquifers consisting of other rock types (Fig. 11).

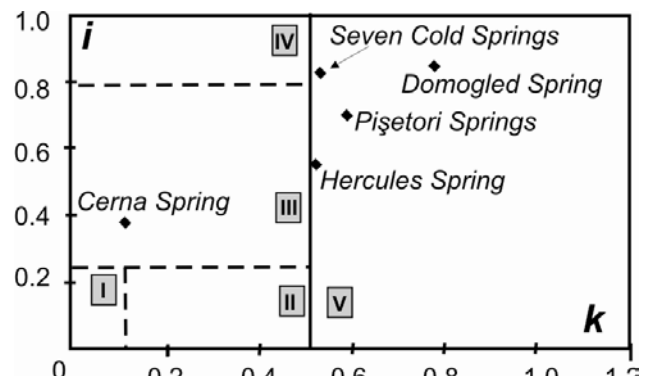


Figure 11. Karst aquifers within the Cerna River catchment, classified according to the correlation between the spectral analysis results: I. outlet caves; II. inlet caves; III. aquifers presenting a stronger karst behavior in the upstream sector, resulting in a delayed recharge; IV. composite aquifers; V. aquifers with non-karst behavior. The non-dimensional coefficients *i* and *k* were retrieved from Povară, 2012.

A conceptual model of the hydrothermal aquifer functioning was set up considering the physical-chemical properties of the water and the geological features (Fig. 12). In terms of chemistry, two basic groundwater types can be recognized within the Cerna river catchment area: on the one hand, there are the waters of the previously described karst systems, while on the other, there is the water of the thermo-mineral aquifer (Table 1).

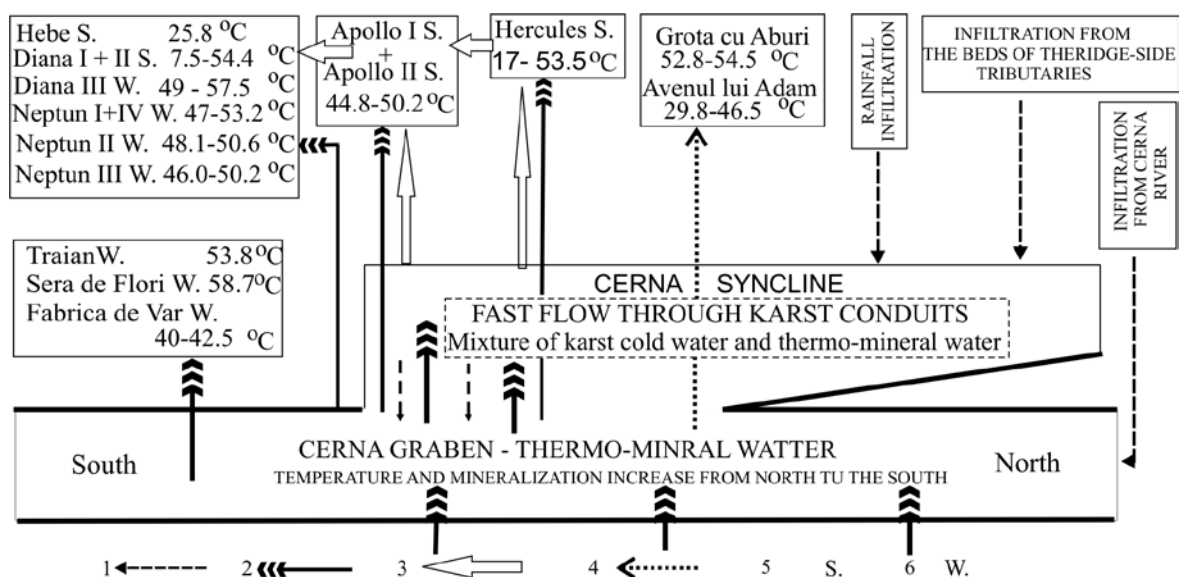


Figure 12. 1. Rainfall infiltration and streambed seepage; 2. thermal and mineralized water input; 3. mixed water; 4. water vapors; 5. natural spring; 6. well (after Povară, 2012, modified).

The first category exhibits the typical characteristics of karst water, namely a low TDS content dominated by the  $\text{Ca}^{2+}$  and  $\text{HCO}_3^-$  ions (the calcium bicarbonate water type - Fig. 13), as well as slightly alkaline pH values. Only very small differences are recorded in terms of chemistry between the various karst systems analyzed in that area: such differences are mainly a result of the duration of the contact between the water and the limestone, as well as of the underground flow type. Although being a surface water, Cerna river assumes the characteristics of a karst water, since it flows over carbonate rocks.

The thermo-mineral water is of sodium chloride type (Fig. 13), has large mineralizations and pH values ranging from neutral to slightly alkaline. Different from the karst systems waters - which in terms of hydrochemistry are largely similar to one another - important distinctions are noticeable between the different thermo-mineral water discharges. Specifically, outflows located in the northern part of the area (the well Crucea Ghizelei, the Seven Warm Springs, the well Scorillo) have smaller mineralizations as compared to the outflows located in the central part of Băile Herculane resort (the springs Apollo II, Hebe), while the outflows located in the southern part of the thermo-mineral water accumulation (the groups of

wells and springs Diana, Neptun, Venera, Traian) are the most strongly mineralized. In fact, the thermal water TDS content increases from the northern part of the aquifer toward the south, from about 300 mg/L, to more than 8000 mg/L.

When the  $\text{Na}^+$  concentration of thermal waters is plotted against the concentration of the conservative constituent  $\text{Cl}^-$  (Fig. 14), there can be noticed that the experimental data-points are rather tightly aligned.

Also the  $\text{H}_2\text{S}$  vs.  $\text{Cl}^-$  correlation is, for most thermal outlets, linear. Yet discharges located toward the thermal aquifer extremities - namely those occurring northward of the spring Apollo II, as well the southernmost wells, Sera de flori and Fabrica de var - deviate from the linear trend. When considering also the sulfate ( $\text{SO}_4^{2-}$ ) anion concentrations indicated in Table 1, it becomes noticeable that the outflows with the lowest  $\text{H}_2\text{S}$  concentrations display, as a general rule, the highest concentrations of  $\text{SO}_4^{2-}$ . This circumstance suggests that while a single  $\text{H}_2\text{S}$  generation mechanism operates within the entire thermal water accumulation, oxidation to sulfate is different from one discharge point to another, as a result of local flow conditions.

Table 1. Average chemical data for the water samples collected from the Cerna River catchment area (mg/L).

Sampling site	n <sup>†</sup>	T (°C)	pH	TDS*	H <sub>2</sub> S	Na	K	Mg	Ca	HCO <sub>3</sub>	SO <sub>4</sub>	Cl
Cerna River	9	15.3	6.57	85	–	3.6	0.9	1.5	26.1	79.2	10.7	2.8
Karst systems												
Cerna Spring	1	10.0	7.67	90	–	2.0	0.3	1.0	31.1	97.7	5.6	0.7
Pișetori Springs	8	8.8	7.78	178	–	1.5	0.6	1.1	64.5	184.9	9.5	1.1
Seven Cold Springs	7	9.9	7.66	155	–	3.5	n.a.	1.9	54.7	175.1	6.5	1.2
Domogled Spring	18	n.a. <sup>‡</sup>	7.61	182	–	0.9	0.9	2.9	62.8	184.7	21.1	1.5
Thermal sources												
Crucea Ghizelei Well	14	31.5	6.69	170	–	1.1	0.4	8.8	53.6	197.6	7.7	1.3
Seven Warm Springs (left)	4	40.4	7.29	551	4.8	169.0	4.9	0.2	22.9	77.0	98.3	217.5
Scorilo Well	14	51.7	7.62	626	6.5	200.5	7.0	0.1	21.6	64.0	102.2	262.6
Hercules Spring	25	45.1	6.95	2661	–	611.1	27.5	3.2	372.9	95.6	97.9	1494.3
Hercules mining Gallery	25	42.8	7.03	2631	–	609.3	24.7	3.2	365.7	95.8	99.2	1474.1
Apollo II Spring	14	47.1	7.24	2408	3.8	605.0	26.4	2.0	292.1	53.1	93.4	1361.1
Hebe Spring	4	25.3	6.65	1321	12.1	279.7	11.8	9.1	208.9	217.0	40.1	668.0
Diana III Well	14	50.0	7.43	2951	27.7	795.3	32.4	1.1	320.6	97.7	23.4	1727.4
Diana I+II Springs	14	53.6	7.06	4851	37.6	1186.9	49.4	2.3	615.0	119.8	13.8	2919.0
Neptun II Spring	14	51.2	7.15	5617	42.9	1365.5	49.4	2.2	730.9	129.3	25.9	3373.5
Neptun III Spring	14	49.9	7.19	5586	26.4	1375.3	49.2	1.4	745.0	81.6	89.8	3277.7
Neptun I + IV Wells	14	55.6	7.13	5618	38.5	1425.8	50.2	2.0	747.9	118.2	38.1	3290.0
Venera Springs	13	38.7	6.96	5526	50.4	1330.0	47.1	3.4	710.4	133.8	11.3	3353.5
Traian Well	14	53.6	7.15	7095	45.7	1681.8	58.0	3.9	970.8	131.2	13.1	4294.7
Sera de Flori Well	14	59.1	7.32	7322	19.0	1708.0	63.4	1.6	1042.0	67.8	150.0	4314.0
Fabrica de Var Well	4	39.8	7.82	7979	33.1	1912.3	56.0	5.8	1134.7	87.7	11.7	4804.0

<sup>†</sup>n = number of samples; \*TDS = total dissolved solids (the sum of the major ions concentrations, with bicarbonate converted to equivalent carbonate); <sup>‡</sup>n.a. = not analyzed.

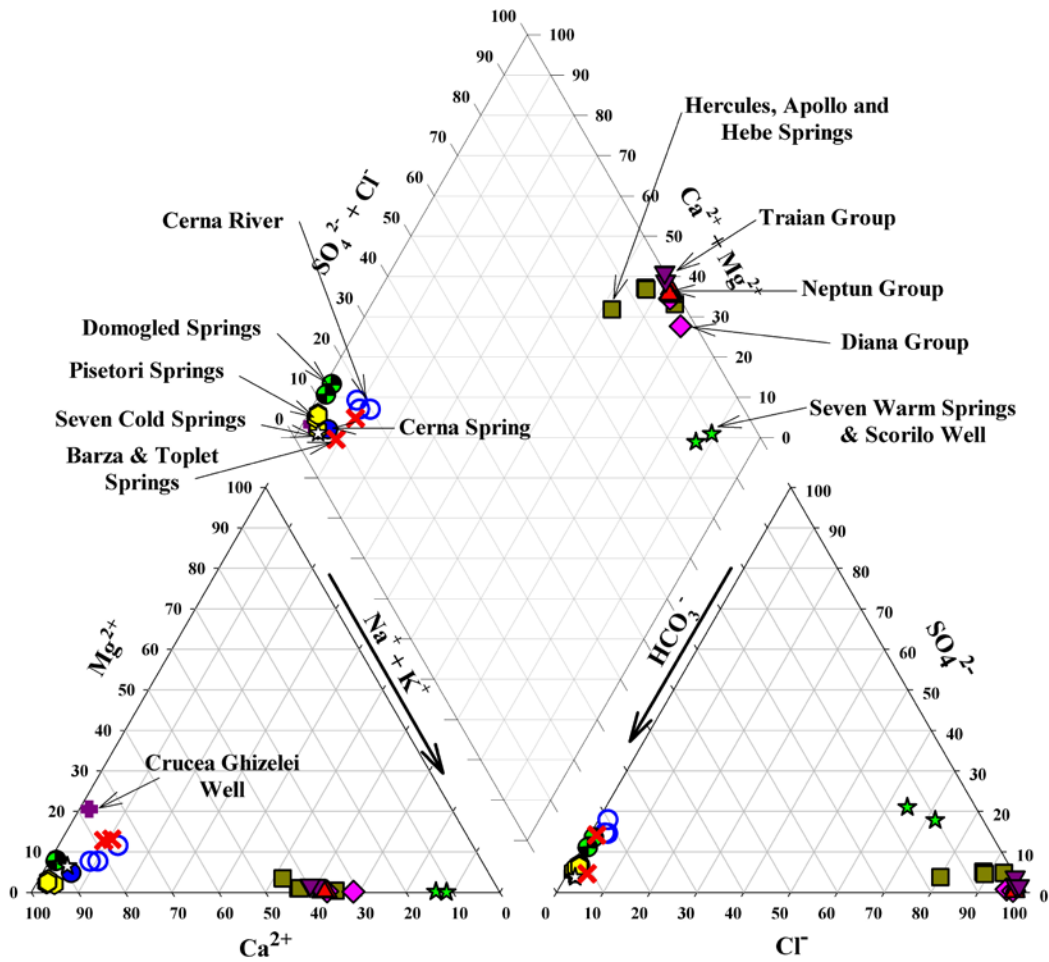


Figure 13. Piper diagram illustrating the hydrochemical facies of various water types from the Cerna River catchment area. There is a clear-cut distinction between the karst (calcium bicarbonate) water and the thermo-mineral (sodium chloride) water.

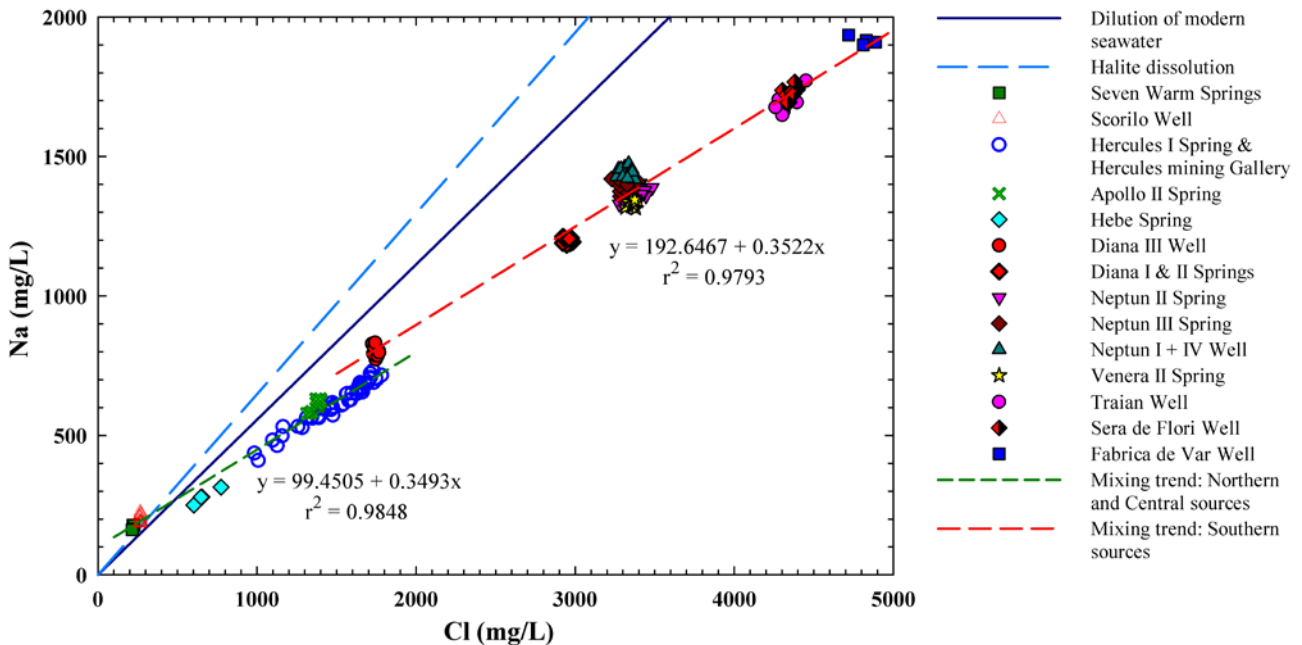


Figure 14. Plot of  $\text{Na}^+$  versus  $\text{Cl}^-$  for the analyzed thermal water. The very good fit of the linear regression lines to the experimental data points suggests that the considered ion concentrations are almost exclusively controlled by a binary mixing between a deep-origin saline solution and a more dilute groundwater. Moreover, for the saline end-member, a significant  $\text{Na}^+$  depletion can be inferred with respect to the stoichiometric dissolution of halite, and to a solution derived from the modern seawater dilution.

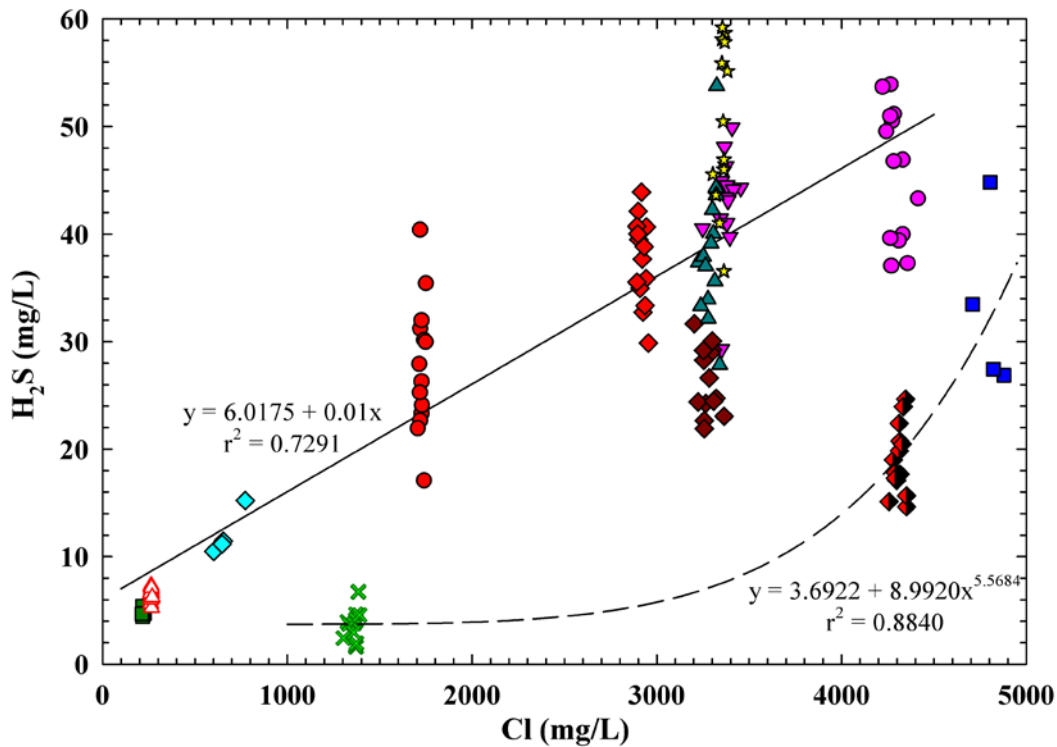


Figure 15. Plot of the dissolved  $H_2S$  versus  $Cl^-$  for the analyzed thermal water. Symbols as in Fig. 14.

## 6. CONCLUSIONS

Extensional structural features influence the karst groundwater flow. Ascending thermo-mineral water outflows within the Cerna Graben, at the intersection of faults related to the graben western fault. Groundwater dye-tracing provided flow velocities varying between 0.15 km/day and 1.6 km/day and allowed the delineation of the main karst springs catchments. The flow duration and the spring flow rate/rainfall correlation analysis highlighted the most important karst systems, which can be assigned to two types: systems with a stronger karst behavior in the upstream sector (e.g. the Cerna Spring) and systems with non-karst behavior (e.g. the Seven Cold Springs, the Pişetori Springs, the Domogled Spring, the Hercules Spring).

The chemical analyses of groundwater samples collected from the Cerna river catchment area outline clear differences existing in terms of hydrochemistry between the karst systems outflows and the thermo-mineral water discharges. In groundwater collected from the investigated karst systems  $Ca^{2+}$  is the prevailing cation, while the prevailing anion is  $HCO_3^-$ , which never exceeds 200 mg/L. Those features are characteristic to groundwater having been in contact with carbonate rocks subject to karst processes. At the same time, only minor differences exist between the waters of the various investigated karst systems. The thermo-mineral water is of Na-Cl type, its mineralization

exhibiting a markedly increasing trend from north to the south. There is an obvious correlation between the concentrations of  $Na^+$  and  $Cl^-$ , this circumstance indicating a process of mixing between a common saline endmember and less mineralized shallow water. The presence of dissolved  $H_2S$ , in concentrations that increase – in a similar way – from north to the south, is another characteristic of the Băile Herculane hydrothermal system. The karst flow influence on the quality of the discharged thermal water is strongly felt at the spring Hercules I and, to a smaller extent, at the springs located immediately to the south, namely Apollo II and Hebe. The significant inflow of karst water induces, especially at the spring Hercules, severe reductions of the water mineralization, episodic alterations of the hydrochemical facies (from Na-Cl to Na- $HCO_3$ ), as well as a complete oxidation of  $H_2S$  into  $SO_4^{2-}$ .

## ACKNOWLEDGEMENTS

This work was supported by a grant from the Romanian National Authority for Scientific Research, CNDS-UEFISCDI, project number PN-II-PT-PCCA-2011-3.1-1619 (Contract No. 48/2012). We gratefully acknowledge the dedicated support provided by Elisabeta Primejdie and Socrate Bucur during the field operations. We are also grateful to Dr. Alin Tudorache and Floarea Răducă for their continuing assistance to the laboratory work, and to Dr. Andrei Giurginca for reviewing the English version of the manuscript.

## REFERENCES

- Aminot, A.**, 1974. *Géochimie des eaux d'aquifères karstiques. II. Les analyses chimiques en hydrogéologie karstique*. Ann. Spéléol., 29-4, 461-483.
- Cline, J.D.**, 1969. *Spectrophotometric determination of hydrogen sulfide in natural waters*. Limnol. Oceanogr., 14, 454-458.
- Conovici, M., Povară, I., Orășeanu, I. & Marin, C.**, 2013. *Geological and hydrogeological features of Cerna Valley (Arșasca-Iuta Area, SW Romania)*. Carpathian Journal of Earth and Environmental Sciences, 8-3, 219-230.
- EPA**, 2007. *Method 6020A. Inductively Coupled Plasma - Mass Spectrometry*. U.S. Environmental Protection Agency.
- Hem, J.D.**, 1985. *Study on interpretation of the chemical characteristics of natural water*. Tech. Rep., U.S. Geological Survey Water-Supply Paper, Vol. 2254, Chap. Evaluation of water composition, 42-57.
- Mangin, A.**, 1975. *Contribution a l'étude hydrodynamique des aquifères karstiques*. Ann. Speleol., 9-3, 283-332; 29-4, 495-601; 30-1, 21-124.
- Mangin, A.**, 1982. *Determination du comportement hydrodynamique des aquifères karstiques à partir de l'étude des informations fournies par leurs exutoires*. Colloque National en Hommage à Castany, Orleans la Source, 397-403.
- Mitrofan, H., Povară, I. & Maftciu, M.**, 2008. *Geoelectrical investigations by means of resistivity methods in karst areas in Romania*. Environmental Geology, 55, 405-413.
- Mitrofan, H. Marin, C. & Povara, I.** 2014. *Possible conduit-matrix water exchange signatures outlined at a karst spring*. Groundwater. doi: 10.1111/gwat.12292
- Niculescu, Gh.**, 1965. *Godeanu Mountains. Geomorphological Study*. Ed. Acad. R.P.R., București, 240 p.
- Năstăseanu, S.**, 1980. *Géologie de Monts Cerna*. An. Inst. Geol. Geofiz., LIV, 153-280.
- Ponta, G., Aldica, Gh., Bădescu, D., Panaiotu C. & Solomon A.**, 1984a. *Speleological researches in Jiul de Vest-Cerțișoara area*. Buletin Speologic FRTA/CCSS, 8, 77-119.
- Ponta, G., Strusiewicz, R., Simion, G. & Gașpar, E.**, 1984b. *Subterranean stream piracy in the Jiul de Vest-Cerțișoara karst area - Romania*. Theor. Appl. Karstology, 1, 235-238.
- Povară, I.**, 2012. *Cerna Valley. Morphology, Hidrology, Thermo-Mineral Water*. Editura AGIR, București, 304 p.
- Povară, I. & Lascu, C.**, 1978. *Note sur la circulation souterraine de l'eau par le graben de Cerna*. Trav. Inst. Spéol "Emile Racovitza", XVII, 193-197.
- Rounds, S.A.**, 2006. *Alkalinity and acid neutralizing capacity (ver. 3.0)*. In: National Field Manual for the Collection of Water-Quality Data, Vol. 9. U.S. Geological Survey Techniques of Water-Resources Investigations, 1-53.
- Săndulescu, M.**, 1984. *Geotectonics of Romania*, Editura Tehnică, București, 335 p.
- Török-Oance, M. & Ardelean, F.**, 2012. *Object-oriented image analysis for detection of the barren karst areas. A case study: the central sector of the Mehedinți Mountains (Southern Carpathians)*. Carpathian Journal of Earth and Environmental Sciences, 7-2, 249-254.
- Veliciu, S.**, 1978. *Geothermics of the Carpathians area*. An. Inst. Geol. Geofiz., 67, 83-116.
- Geological Map of Romania** 1:200 000 (Baia de Aramă and Târgu Jiu sheets) and 1:50 000 (Oslea Sheet), edited by the Geological Institute of Romania.

Received at: 24. 03. 2014

Revised at: 23.01. 2015

Accepted for publication at: 23. 02. 2015

Published online at: 28. 02. 2015